

Article

Thermochromic Behavior of VO₂/Polymer Nanocomposites for Energy Saving Coatings

Michalis Xygkis ^{1,2}, Emmanouil Gagaoudakis ^{1,2}, Leila Zouridi ^{1,3}, Olga Markaki ^{1,2}, Elias Aperathitis ¹, Kyriaki Chrissopoulou ¹ , George Kiriakidis ^{1,2}  and Vassilios Binas ^{1,4,*} 

¹ Institute of Electronic Structure and Laser, Foundation for Research and Technology Hellas 100 N, Plastira str., Vassilika Vouton, 70013 Heraklion, Crete, Greece; ph4213@edu.physics.uoc.gr (M.X.); mgagas@iesl.forth.gr (E.G.); l.zouridi@iesl.forth.gr (L.Z.); ph4308@edu.physics.uoc.gr (O.M.); eaper@iesl.forth.gr (E.A.); kiki@iesl.forth.gr (K.C.); kiriakid@iesl.forth.gr (G.K.)

² Department of Physics, University of Crete, 71003 Heraklion, Crete, Greece

³ Department of Material Science & Technology, University of Crete, 71003 Heraklion, Crete, Greece

⁴ Department of Physics, Crete Center for Quantum Complexity and Nanotechnology, University of Crete, 71003 Heraklion, Crete, Greece

* Correspondence: binasbill@iesl.forth.gr; Tel.: +2810-391269

Received: 19 January 2019; Accepted: 22 February 2019; Published: 1 March 2019



Abstract: Vanadium dioxide (VO₂) is a well-known thermochromic material that can potentially be used as a smart coating on glazing systems in order to regulate the internal temperature of buildings. Most growth techniques for VO₂ demand high temperatures (>250 °C), making it impossible to comply with flexible (polymeric) substrates. To overcome this problem, hydrothermally synthesized VO₂ particles may be dispersed in an appropriate matrix, leading to a thermochromic coating that can be applied on a substrate at a low temperature (<100 °C). In this work, we reported on the thermochromic properties of a VO₂/Poly-Vinyl-Pyrrolidone (PVP) nanocomposite. More specifically, a fixed amount of VO₂ particles was dispersed in different PVP quantities forming hybrids of various VO₂/PVP molar ratios which were deposited as films on fused silica glass substrates by utilizing the drop-casting method. The crystallite size was calculated and found to be 35 nm, almost independent of the PVP concentration. As far as the thermochromic characteristics are concerned, the molar ratio of the VO₂/PVP nanocomposite producing VO₂ films with the optimum thermochromic properties was 0.8. These films exhibited integral solar transmittance modulation (overall wavelengths) $\Delta Tr_{sol} = 0.35\% - 1.7\%$, infrared (IR) switching at 2000 nm $\Delta Tr_{IR} = 10\%$, visible transmittance at 550 nm $Tr_{vis} = 38\%$, critical transition temperature $T_C = 66.8\text{ }^\circ\text{C}$, and width of transmittance hysteresis loop $\Delta T_C = 6.8\text{ }^\circ\text{C}$. Moreover, the critical transition temperature was observed to slightly shift depending on the VO₂/PVP molar ratio.

Keywords: hydrothermal synthesis; thermochromic VO₂; low-temperature VO₂/PVP nanocomposites; thermochromic coatings

1. Introduction

Versatile solutions to the expanding and rapid increase in worldwide energy demands as well as the restrictions concerning environmental pollution by utilizing renewable energy sources and energy-efficient materials have already attracted both scientific interest and commercial attention. The energy consumption in buildings alone is estimated to be approximately 40% of the world's total energy consumption, and it is anticipated it will increase steadily [1–3]. Central heating, ventilation, and air conditioning are the main energy consumers, being responsible for about 30% of annual carbon dioxide emissions [3]. Moreover, heat transmittance and insulation inefficiency of windows are responsible for 15%–22% of a building's energy loss [4–7].

In recent years, 'smart' windows have received widespread attention as one of the potential solutions to reducing energy consumption by air conditioning in modern architecture. 'Smart' windows are able to intelligently self-regulate the amount of transmitted heat, while keeping the visible transmission mainly unchanged. Vanadium dioxide (VO_2) is one of the most promising solid-state materials for smart windows due to its unique optical properties related to its inherent and ultrafast reversible structural (phase-change) transition from a monoclinic $\text{VO}_2(\text{M})$ to tetragonal rutile $\text{VO}_2(\text{R})$ structure at a critical transition temperature of $T_C = 68^\circ\text{C}$, for pure monocrystalline material [8–10].

Conventionally, 'smart' thermochromic windows are fabricated by vapor phase deposition techniques such as sputtering [11–14], chemical vapor deposition (CVD) [15–17], and pulsed laser deposition (PLD) [18]. However, all these techniques are restricted by the cost and scale of vacuum systems. Moreover, most of these growth techniques, although they are of high fidelity and can produce good quality thermochromic VO_2 films, demand high deposition temperatures ($>400^\circ\text{C}$) [11,14–18], with very few employing sputtering techniques between 250 and 300 $^\circ\text{C}$ [12,13,19–21], making it impossible to utilize flexible (polymeric) substrates.

Another approach, called the ex-situ approach [22], to the fabrication of VO_2 thermochromic films is to first synthesize the desired material as a powder and then to deposit the material as a film onto the desired surface. Thermochromic VO_2 in the form of powders have been synthesized by various methods, such as thermolysis [23,24], rapid thermal annealing [25], pyrolysis [26], and, the most utilized method, hydrothermal (solvothermal) synthesis [27–31]. The latter is the most promising due to the high crystallinity of the resulting products, the precise phase control, the versatility on the synthetic parameters, and the possibility of large-scale synthesis [32].

In order to transform the powder into film, various deposition methods have been applied, most notably sol-gel methods. Sol-gel is a proper inexpensive method for large-scale deposition, utilizing fast processing techniques such as dip and spin coating [33]. In particular, the sol-gel method is suitable for the deposition of VO_2 , either directly on rigid or on flexible substrates (membrane) attached to glass surfaces. In the sol-gel method, a mixture of a precursor-supporting material along with the particles of the functional material are used (e.g., usually a polymer or monomer along with VO_2 particles) in order to synthesize the films [33–35]. Hence the polymer has to be adequately selected to fulfill several demands, including: (i) Stabilization of the VO_2 particles dispersion, (ii) prevention of agglomerations, and (iii) protection of VO_2 particles, e.g., from oxidation/reduction by air or water vapor, which is especially important during the long storage period. Among the various prospective polymeric host matrices, such as polyoxymethylene, polyvinyl alcohol, polyacrylic acid, etc., the one fulfilling the above criteria to a fairly satisfying level has been identified to be Poly-Vinyl-Pyrrolidone (PVP) [36]. Although the sol-gel process is a promising technique for achieving a low deposition temperature for thermochromic VO_2 film fabrication, various concerns such as thickness control and repeatability have not yet been met equivalently in all the different deposition methods used (spin-coating, drop-casting, dip-coating, and spraying), thus sustaining the interest of the research community and industry [37,38].

In the present work, thermochromic VO_2 /polymer nanocomposite films were deposited uniformly using a casting method on glass substrates. The method selected was polymer-assisted deposition employing the drop-casting technique. The polymer utilized was PVP. A parametric study was carried out in order to examine the effect of the VO_2 /PVP molar ratio on the thermochromic properties. The quantities of both the dispersant (distilled water) and the VO_2 particles were kept constant, while the quantity of PVP was varied, in order to change the molar ratio of VO_2 /PVP. It is the first time that such a study has been performed, since until now the majority of research [39–44] has mainly focused on the thermochromic behavior of VO_2 powder/composite, without showing how the thermochromic properties are affected by the presence of a host material.

2. Materials and Methods

2.1. Synthesis of VO₂ Particles

The reagents used were vanadium pentoxide, V₂O₅ (+98% pure), as the vanadium source and oxalic acid dihydrate, H₂C₂O₄·2H₂O (≥99.0% pure), as the reducing agent. All reagents were purchased from Sigma Aldrich (Merck, Germany) and were used without further purification.

VO₂ particles were synthesized via a typical hydrothermal procedure using a Parr Teflon-lined stainless steel autoclave. In a typical procedure, 2 mmol of V₂O₅ powder and 8 mmol of H₂C₂O₄·2H₂O were dissolved in 2.22 mol of deionized water, resulting in a 32 vol% filling of the Teflon vessel. After stirring, the original dark yellow mixture turned into a dark green-blue solution. For the hydrothermal treatment, the precursor mixture was transferred to the acid digestion vessel and into a furnace for treatment at 220 °C for 12 h. The obtained blue-black solid product was isolated via centrifugation, after drying at 80 °C for 4 h. Finally, to acquire the desired crystalline phase of thermochromic VO₂ the solid product was annealed at 700 °C for 2 h under a constant nitrogen gas flow.

2.2. VO₂/Polymer Nanocomposite Coatings

The as-prepared VO₂ particles were dispersed ultrasonically in deionized water at a concentration of 10 mg/mL for 30 min and stirred for 1 h to produce a suspension. Then, an appropriate amount of PVP K-30 was added in different molar ratios of VO₂/PVP, from 0.2 to 1.2, by decreasing the amount of PVP while keeping constant the amount of VO₂ particles. The suspension was stirred for 2 h to enhance its homogeneity. Prior to the deposition, fused silica glass substrates were treated with ethanol and propanol inside a sonication bath for 5 min, respectively. Finally, the mixture was uniformly casted on the substrates and dried for 1 h at 70 °C.

2.3. Structural and Morphological Characterization/Thermochromic Properties

The structural characterization of VO₂ particles and nanocomposite films was performed by X-ray diffraction (XRD) using a Rigaku RINT-2000 diffractometer (Tokyo, Japan). The X-rays were produced by a 12 kW rotating anode generator with a Cu anode equipped with a secondary pyrolytic graphite monochromator. A Cu K α radiation with wavelength $\lambda = 0.154$ nm was used. Measurements were performed with $\theta/2\theta$ configuration, scanning from 20° to 80° with a step of 0.02°/min. The crystallite size of the VO₂ was calculated by using the Scherrer Equation;

$$d(\text{nm}) = \frac{0.9 \cdot \lambda(\text{nm})}{B \cdot \cos(\theta_B)} \quad (1)$$

where $\lambda = 0.154$ nm, B the full width at half maximum (FWHM) at $2\theta = 27.8^\circ$ corresponding to the characteristic (011) direction of the VO₂ peak, and $\theta_B = \theta$.

The morphology of the VO₂ particles and nanocomposite films was determined by scanning electron microscopy (SEM, JEOL 7000, Tokyo, Japan) operating at 15 keV, while the microscopic nanostructures were observed by transmission electron microscopy (TEM) on a JEM-2100 instrument (JEOL, Tokyo, Japan) equipped with LaB₆ filament, operating at 200 kV.

The critical transition temperature of the VO₂ particles was determined by differential scanning calorimetry (DSC) using a PL-DSC system from Polymer Laboratories. Measurements were performed from 20 to 170 °C and back to 20 °C with a step of 10 °C/min, under a nitrogen flow of 20 cc/min. By identifying the critical transition temperature during heating (T_1) and cooling (T_2) procedures, the critical transition temperature (T_C) as well as the width of the hysteresis loop of the VO₂ powder were calculated as defined by the Equations below:

$$T_C = \frac{T_1 + T_2}{2} \quad (2)$$

$$\Delta T_C = T_1 - T_2 \quad (3)$$

The thermochromic properties of the nanocomposite films were examined by recording the transmittance spectra in the temperature range of 25 and 90 °C. For this, a Perkin Elmer Lambda 950 UV/Vis/NIR spectrophotometer, operating at $\lambda = 250\text{--}2500$ nm with a homemade heating sample stage attachment and a thermocouple on contact with the surface of the film to measure the temperature, was used. The temperature was controlled by an ACUSHNET FP-900 temperature controller (Taipei, Taiwan) at a heating rate of 1.5 °C/min. IR switching is defined as the difference of transmittance value at $\lambda = 2000$ nm, between 25 and 90 °C.

$$\Delta Tr_{IR} (\%) = Tr_{IR}(25 \text{ } ^\circ\text{C}) - Tr_{IR}(90 \text{ } ^\circ\text{C}) \quad (4)$$

while integral luminous transmittance is defined as:

$$Tr_{lum} (\%) = \frac{\int_{350}^{750} B_{lum}(\lambda) * Tr(\lambda) d\lambda}{\int_{350}^{750} B_{lum}(\lambda) d\lambda} \quad (5)$$

where $Tr(\lambda)$ is the recorded transmittance spectrum at 25 or 90 °C and $B_{lum}(\lambda)$ is the standard luminous efficiency function for photopic vision [45].

Moreover, solar transmittance modulation $\Delta Tr_{sol} (\%)$ is defined as the difference of integral solar transmission between 25 and 90 °C, obtained by the formula:

$$\Delta Tr_{sol} (\%) = \frac{\int_{250}^{2500} B_{sol}(\lambda) * Tr(T = 25 \text{ } ^\circ\text{C}, \lambda) d\lambda - \int_{250}^{2500} B_{sol}(\lambda) * Tr(T = 90 \text{ } ^\circ\text{C}, \lambda) d\lambda}{\int_{250}^{2500} B_{sol}(\lambda) d\lambda} \quad (6)$$

where $Tr(\lambda)$ is the recorded transmittance spectrum at 25 or 90 °C and $B_{sol}(\lambda)$ is the solar irradiance spectrum for an air mass (AM) of 1.5 (corresponding to a solar zenith angle of 48.2° [46]).

Furthermore, in order to determine the critical transition temperature of VO₂/polymer nanocomposite films through optical measurements, the transmittance as a function of temperature (25–90 °C) by a step of 1.5 °C/min at $\lambda = 2000$ nm was recorded for both the heating and cooling procedure. The derivative of transmittance (dTr/dT) versus temperature was plotted and fitted by a Gaussian curve for both procedures. The minimum of the fitting curves determined the critical transition temperature T_1 and T_2 for the heating and cooling procedure, respectively. Thus, the critical transition temperature T_C and the width of transmittance hysteresis loop were obtained by Equations (2) and (3), respectively.

3. Results and Discussion

3.1. Structural and Morphological Characterization of VO₂ Particles

Figure 1a shows the XRD pattern of VO₂ powder particles (for $2\theta = 20\text{--}80^\circ$), from which the monoclinic phase of VO₂ (M) is confirmed (JCPDS card No. 43-1051). The crystallite size of the VO₂ powder was calculated from the XRD pattern using Scherer's Equation (Equation (1)) and was found to be around 35 nm. TEM imaging revealed the material to be composed of nanoflakes, with particles varying from less than 25 to 400 nm, as presented in Figure 1e,f. The thermochromic behavior of the VO₂ particles was confirmed by the DSC diagram of Figure 1b, from which the critical transition temperature and the hysteresis width were calculated and found to be $T_C = 66.6$ °C and $\Delta T_C = 12.1$ °C. The morphology of the VO₂ particles was investigated by SEM, presented in Figure 1c,d, in which nanoflake agglomerates with sizes up to about 500 nm can be observed.

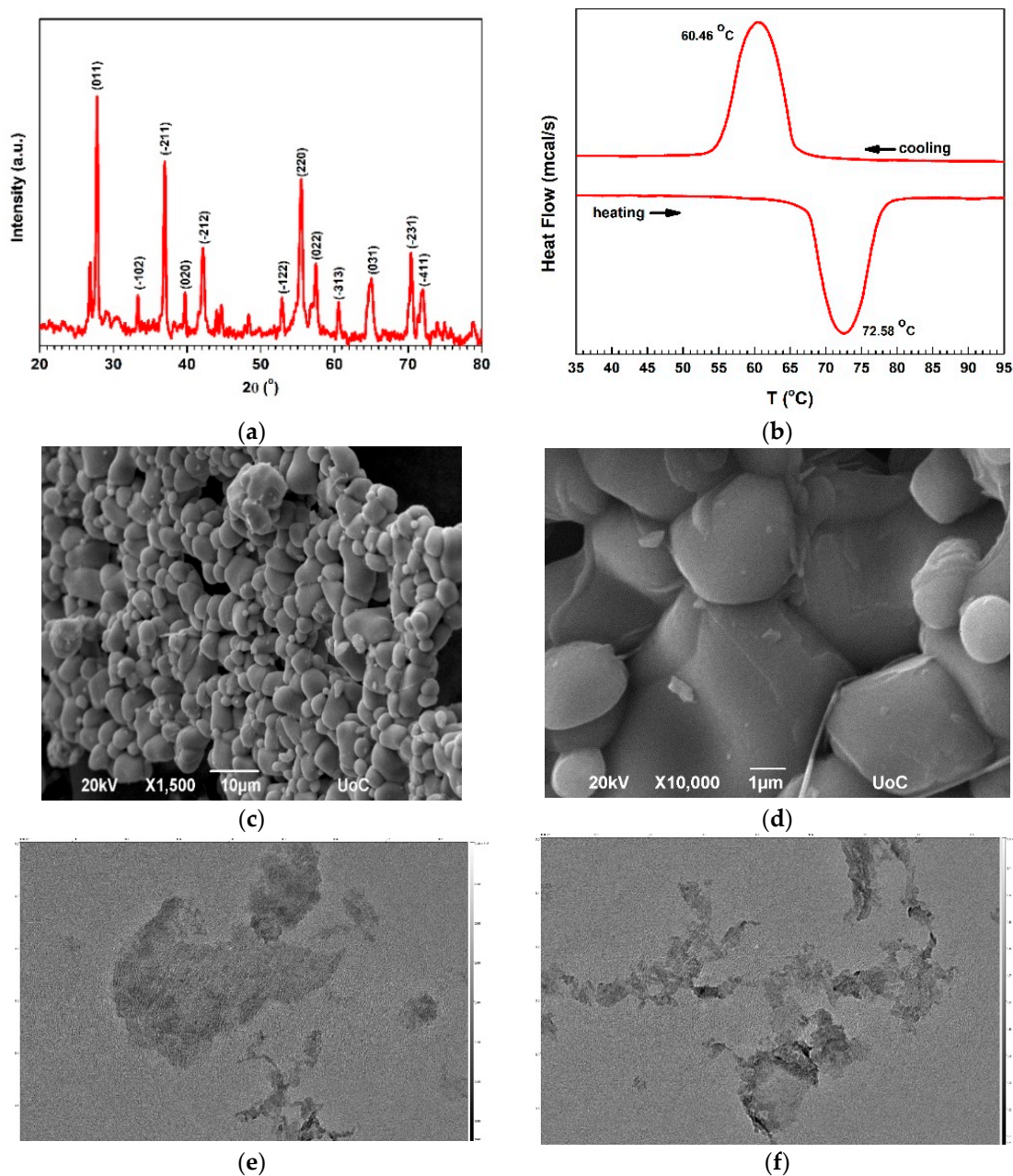


Figure 1. (a) XRD pattern; (b) differential scanning calorimetry (DSC) curve; (c,d) SEM images, and (e,f) TEM images of VO_2 powder particles.

3.2. Structural and Morphological Characterization of VO_2 /Polymer Nanocomposite Films

The XRD pattern of VO_2 /polymer nanocomposite films at the optimized ratio of $\text{VO}_2/\text{PVP} = 0.8$ deposited on fused silica glass substrate is shown in Figure 2a, along with a picture of the film in Figure 2b. The monoclinic phase of VO_2 was confirmed by the two characteristic peaks at $2\theta = 27.8^\circ$ and 37.0° corresponding to the VO_2 (011) and (200) crystallographic directions, respectively, according to JCPDS card No. 44-0252. The small peak at around 25° is attributed to the glass substrate. Thus, the polymer PVP does not affect the crystallinity of the VO_2 . In addition, the crystallite size of VO_2 in the composite was calculated and found to be the same (35 nm) as that of VO_2 in powder form. However, the rest of the peaks corresponding to the VO_2 powder (Figure 1a) could not be detected in the composite, probably due to the presence of the host material (PVP).

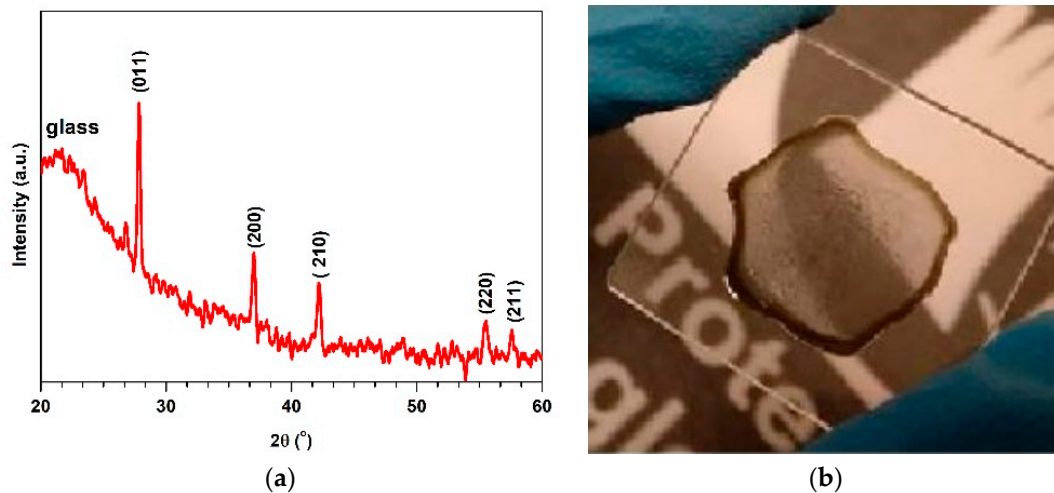


Figure 2. (a) XRD pattern and (b) image of VO_2 /Poly-Vinyl-Pyrrolidone (PVP) nanocomposite film with ratio $\text{VO}_2/\text{PVP} = 0.8$ deposited on fused silica substrate.

In order to investigate the effect of the amount of PVP in the morphology of the surface of VO_2 /polymer nanocomposite films, SEM at $\times 1500$ magnification was performed. VO_2 particles, as shown in Figure 3, were found to have almost entirely been submerged, particularly at the optimized ratio of $\text{VO}_2/\text{PVP} = 0.8$, within the polymer matrices exhibiting a smooth composite finish surface without cracks. Moreover, it was found that the presence of polymer for all ratios from 0.2 to 1 prevented the agglomeration of particles with an average grain size of more than 500 nm.

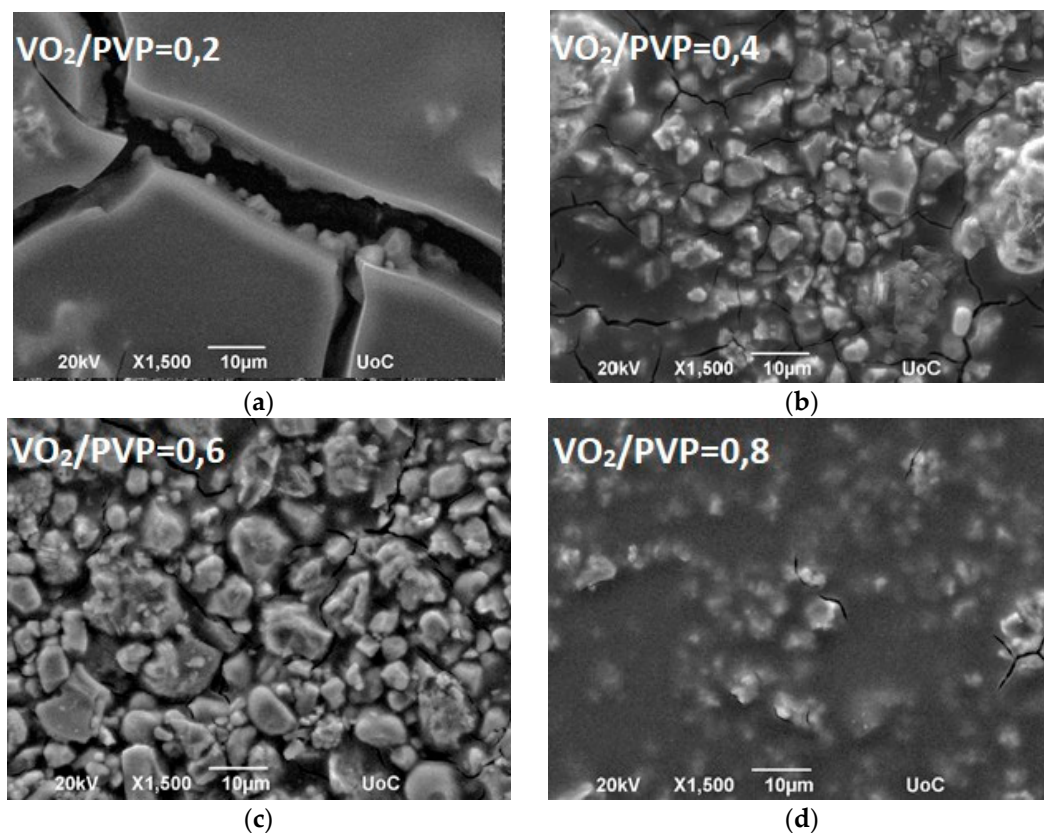


Figure 3. Cont.

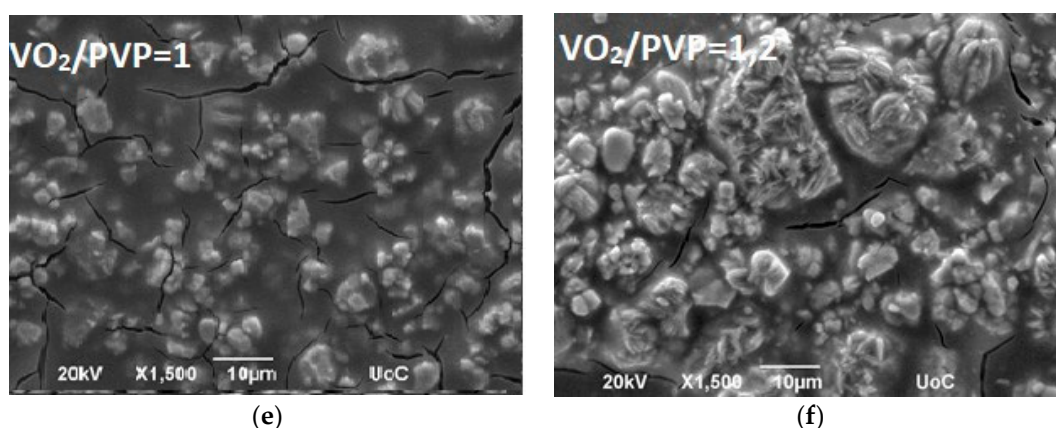


Figure 3. SEM images of VO₂/PVP nanocomposite films with a different molar ratio of VO₂: PVP from 0.2 to 1.2.

3.3. Effect of VO₂/PVP Molar Ratio on Thermo-chromic Properties

The transmittance spectra from 250 to 2500 nm of VO₂/polymer nanocomposite films with a different VO₂/PVP molar ratio at 25 and 90 °C are presented in Figure 4a–d. It can be seen that all films exhibit a thermo-chromic behavior. Utilizing these spectra along with Equations (4)–(6) IR switching at 2000 nm, Tr_{lum} and Tr_{sol} were calculated and are presented in Table 1.

Table 1. Optical characteristics of VO₂/polymer nanocomposite films.

VO ₂ /PVP *	Tr_{lum} (%)	ΔTr_{IR} (%)	ΔTr_{sol} (%)
0.2	24.5	7	1.72
0.4	27.2	5.7	0.36
0.6	26.9	7.8	1.00
0.8	37.1	10.2	1.22
1	36.8	7.8	1.35
1.2	41.2	4.8	0.35

* molar ratio.

According to Table 1, it is clear that the luminous transmittance is decreasing as the concentration of PVP increases (i.e., the ratio of VO₂/ PVP is decreases) due to the anticipated increase of film thickness, varying between 3 and 5 µm, as a result of the casting method. Concerning the effect of PVP on IR switching, there is an optimal ratio of VO₂/PVP = 0.8, for which IR switching becomes maximum and equal to 10.2%, as presented in the graphical representation of data in Figure 5a. Furthermore, the calculated solar transmittance modulation varied from 0.35% to 1.7% without any evident indication on whether there is a correlation with the VO₂/PVP molar ratio, rather than a moderately noticeable non-linear increase of ΔTr_{sol} with the increase of PVP in solution concentration (i.e., a decrease of the VO₂/PVP molar ratio). Although solar transmittance modulation is low enough when compared to thermo-chromic films prepared by other techniques at higher deposition temperatures [1,4,16], a systematic investigation on the dispersion of VO₂ powder in the solvent should lead to an improvement of thermo-chromic characteristics. Additionally, a different casting method such as dip coating or spin coating will be employed in order to increase the homogeneity of the films, resulting in an increase of luminous transmittance.

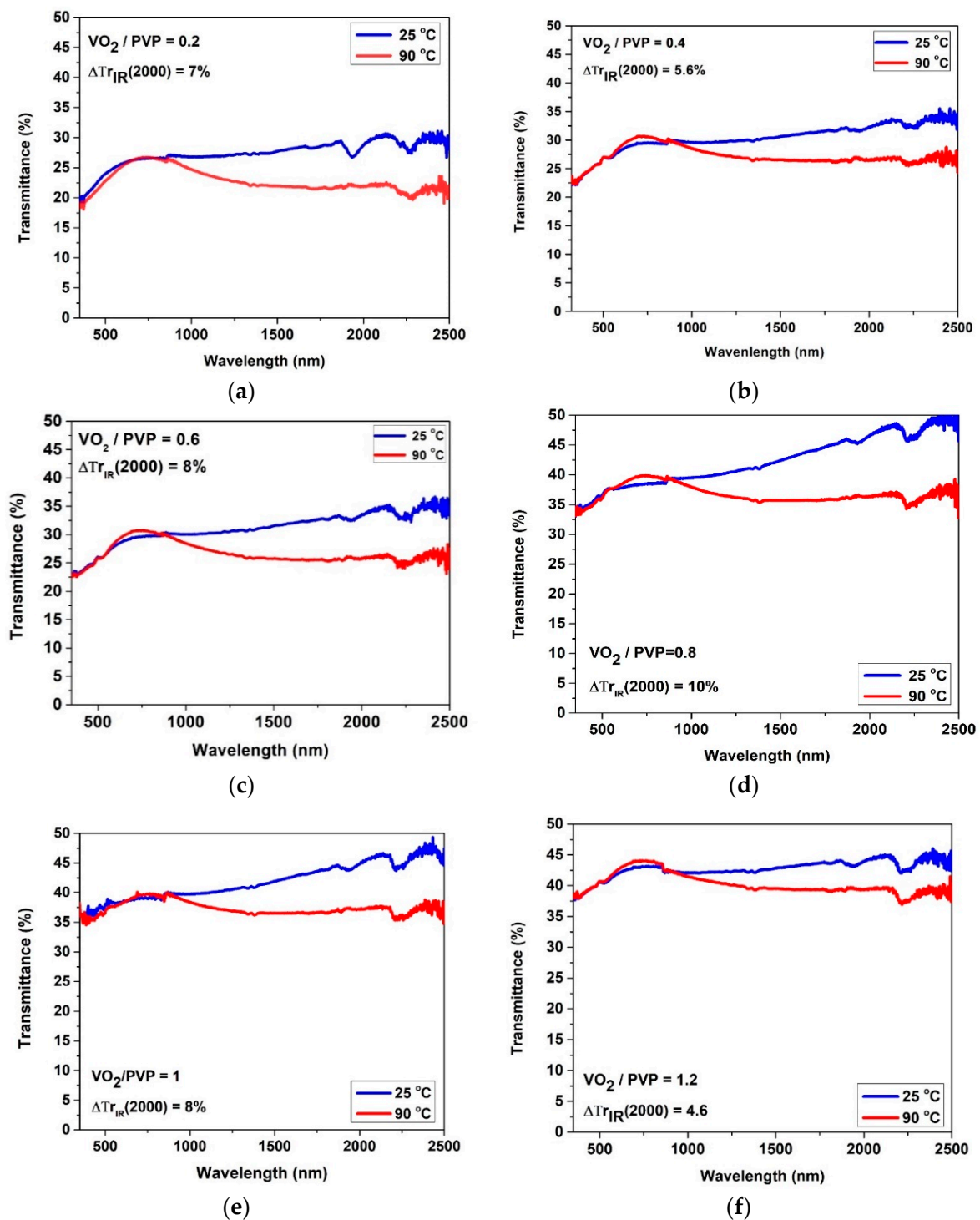


Figure 4. Transmittance spectra at 25 (blue line) and 90 °C (red line) of VO₂/PVP nanocomposite films prepared with different molar ratios of VO₂/PVP: (a) 0.2, (b) 0.4, (c) 0.6, (d) 0.8, (e) 1.0, and (f) 1.2.

The transmittance hysteresis loop of VO₂/PVP nanocomposites with different amounts of PVP, at $\lambda = 2000$ nm is presented in Figure 6. From these heating–cooling loops, it is evident that the transition is a fully reversible process for all VO₂/PVP nanocomposite samples. By using Equations (2) and (3), the critical transition temperature and the hysteresis width, respectively, were calculated. The results are presented in Table 2, while in Figure 5b the variation of T_C is graphically presented as a function of the VO₂/PVP molar ratio. It is observed that T_C is increasing in regards to the molar ratio of VO₂/PVP from 62 °C (VO₂/PVP = 0.2) to 68 °C (VO₂/PVP = 1.2). This behavior can be attributed

to the increasing concentration of polymer in the films (from the 1.2 to the 0.2 VO₂: PVP molar ratio), since a higher polymer concentration seems to inhibit the agglomeration of VO₂ nanoparticles. Thus, the transition is enhanced by reducing the energy needed for VO₂ particles in the film to transition from the monoclinic to the full tetragonal rutile phase (and vice versa), leading to lower T_C values. A similar phenomenon is observed for the width of transmittance hysteresis loop, since it is increased from 3.5 °C for VO₂/PVP = 0.2 to 8.1 °C for VO₂/PVP = 1.2, indicating that the increase of PVP facilitates the transition, thus lowering the hysteresis width.

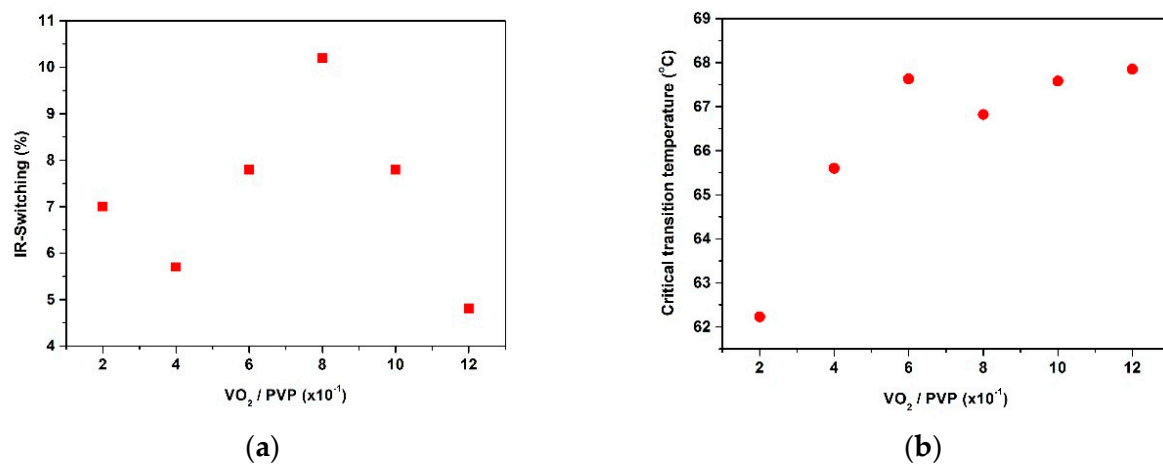


Figure 5. Effect of the VO₂/PVP molar ratio on thermochromic characteristics of VO₂/PVP nanocomposite films. (a) IR switching (ΔT_{IR}), as calculated by Equation (4) at $\lambda = 2000$ nm and (b) critical transition temperature (T_C).

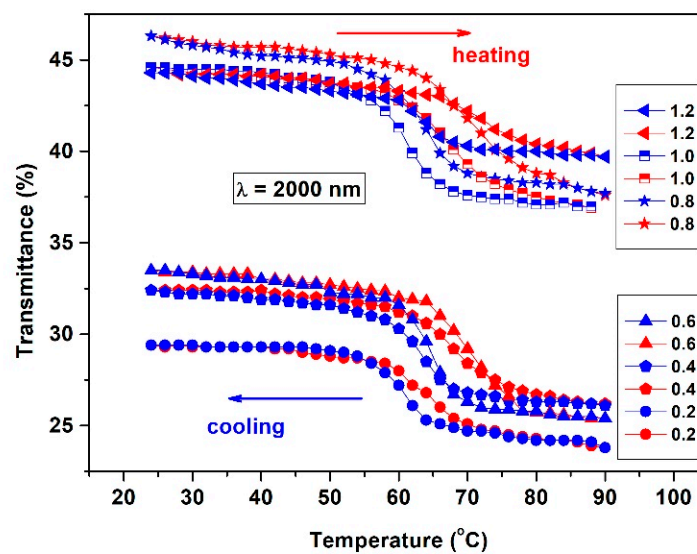


Figure 6. Transmittance hysteresis loop of VO₂/PVP nanocomposite films prepared with different amounts of PVP, recorded at $\lambda = 2000$ nm. Heating (red line), cooling (blue line).

Table 2. Critical transition temperature T_C and width of transmittance hysteresis loop (ΔT_C) of VO₂/PVP nanocomposite films for different amounts of PVP.

VO ₂ /PVP *	ΔT_C (°C)	T_C (°C)
0.2	3.5	62.2
0.4	5.0	65.6
0.6	6.0	67.6
0.8	6.8	66.8
1.0	4.9	67.6
1.2	8.1	67.8

* molar ratio.

4. Conclusions

In this work, hydrothermal synthesis was employed to formulate pure monoclinic VO₂ particles. Subsequently, VO₂/PVP nanocomposite films were fabricated by polymer-assisted deposition on fused silica commercial glass at low treatment temperatures (<70 °C). Both thermochromic and optical properties were examined as a function of the VO₂/PVP molar ratio varying from 0.2 to 1.2, by only changing the amount of PVP in the solution. The IR switching at 2000 nm was found to depend on the molar ratio of VO₂/PVP and the optimal ratio was determined to be 0.8, for which $\Delta Tr_{IR} = 10.2\%$. The integrated luminous transmittance varied from 24.5% to 41.2% as the ratio of VO₂/PVP increased from 0.2 to 1.2 (i.e., the amount of PVP was decreased), probably due to the increase on thickness of the produced films. Additionally, the solar transmittance modulation of the VO₂/PVP nanocomposites non-linearly increased from 0.35% to 1.7% as the amount of PVP increased (i.e., a lower VO₂/PVP molar ratio). Finally, it was observed that the critical transition temperature non-linearly increased from 62.2 to 67.8 °C as the ratio of VO₂/PVP increased. This was attributed to the presence of the polymer which inhibits the agglomeration of the VO₂ particles, resulting in lower T_C values for the transition.

Author Contributions: Conceptualization, E.G. and V.B.; Methodology, L.Z.; Software, M.X.; Validation, L.Z., E.G. and V.B.; Formal Analysis, M.X.; Investigation, O.M.; Data Curation, E.G.; Writing—Original Draft Preparation, M.X.; Writing—Review and Editing, G.K.; E.A. and K.C.; Visualization, E.G.; Supervision, V.B.; Project Administration, V.B.; Funding Acquisition, G.K.

Funding: This research was funded by a research grant from the Hellenic Ministry of Education with the acronym EXOTHERMO (09SYN-32-1185) and Innovation-EL, and the project “Electronics Beyond Silicon Era” (ELBYSIER) Erasmus+ KA2 programme.

Acknowledgments: The authors would like to deeply thank Lampros Papoutsakis and Dora Dragani for their time and effort, which proved crucial for the completion of this work.

Conflicts of Interest: The authors declare no conflict of interest. The funders had no role in the design of the study; in the collection, analyses, or interpretation of data; in the writing of the manuscript, and in the decision to publish the results”.

References

1. Kamalisarvestani, M.; Saidur, R.; Mekhilef, S.; Javadi, F.S. Performance, materials and coating technologies of thermochromic thin films on smart windows. *Renew. Energy Rev.* **2013**, *26*, 353–364. [[CrossRef](#)]
2. Kanu, S.S.; Binions, R. Thin films for solar control applications. *Proc. R. Soc. A* **2010**, *466*. [[CrossRef](#)]
3. United Nations Environment Programme. *Buildings and Climate Change: Summary for Decision Makers*; UNEP: Paris, France, 2017.
4. Long, L.; Ye, H. How to be smart and energy efficient: A general discussion on thermochromic windows. *Sci. Rep.* **2014**, *4*, 6427. [[CrossRef](#)] [[PubMed](#)]
5. Pérez-Lombard, L.; Ortiz, J.; Pout, C. A review on buildings energy consumption information. *Energy Build.* **2008**, *40*, 394–398. [[CrossRef](#)]
6. Chen, X.; Yang, H.; Lu, L. A comprehensive review on passive design approaches in green building rating tools. *Renew. Sustain. Energy Rev.* **2015**, *50*, 1425–1436. [[CrossRef](#)]

7. Al-Rabghi, O.M.; Hittle, D.C. Energy simulation in buildings: Overview and BLAST example. *Energy Convers. Manag.* **2001**, *42*, 1623–1635. [[CrossRef](#)]
8. Morin, F.J. Oxides which show a metal-to-insulator transition at the Neel temperature. *Phys. Rev. Lett.* **1959**, *3*, 34–36. [[CrossRef](#)]
9. Goodenough, J.B. The two components of the crystallographic transition in VO₂. *J. Solid State Chem.* **1971**, *3*, 490–500. [[CrossRef](#)]
10. Chang, T.C.; Cao, X.; Bao, S.H.; Ji, S.D.; Luo, H.J.; Jin, P. Review on thermochromic vanadium dioxide based smart coatings: From lab to commercial application. *Adv. Manuf.* **2018**, *6*, 1–19. [[CrossRef](#)]
11. Luo, Y.Y.; Pan, S.S.; Xu, S.C.; Zhong, L.; Wang, H.; Li, G.H. Influence of sputtering power on the phase transition performance of VO₂ thin films grown by magnetron sputtering. *J. Alloy. Compd.* **2016**, *664*, 626–631. [[CrossRef](#)]
12. Gagaoudakis, E.; Kortidis, I.; Michail, G.; Tsagaraki, K.; Binas, V.; Kiriakidis, G.; Aperathitis, E. Study of low temperature rf-sputtered Mg-doped vanadium dioxide thermochromic films deposited on low-emissivity substrates. *Thin Solid Films* **2016**, *601*, 99–105. [[CrossRef](#)]
13. Gagaoudakis, E.; Aperathitis, E.; Michail, G.; Panagopoulou, M.; Katerinopoulou, D.; Binas, V.; Raptis, Y.S.; Kiriakidis, G. Low-temperature rf sputtered VO₂ thin films as thermochromic coatings for smart glazing systems. *Solar Energy* **2018**, *165*, 115–121. [[CrossRef](#)]
14. Zhu, M.D.; Shan, C.; Li, C.; Wang, H.; Qi, H.J.; Zhang, D.P.; Lv, W. Thermochromic and femtosecond-laser-induced damage performance of tungsten-doped vanadium dioxide films prepared using an alloy target. *Materials* **2018**, *11*, 1724. [[CrossRef](#)] [[PubMed](#)]
15. Vernardou, D.; Louloudakis, D.; Spanakis, E.; Katsarakis, N.; Koudoumas, E. Thermochromic amorphous VO₂ coatings grown by APCVD using a single-precursor. *Sol. Energy Mater. Sol. Cells* **2014**, *128*, 36–40. [[CrossRef](#)]
16. Vernardou, D.; Louloudakis, D.; Spanakis, E.; Katsarakis, N.; Koudoumas, E. Thermochromic vanadium oxide coatings grown by APCVD at low temperatures. *Phys. Proced.* **2013**, *46*, 137–141. [[CrossRef](#)]
17. Lee, W.J.; Chang, Y.H. Growth without postannealing of monoclinic VO₂ thin film by atomic layer deposition using VCl₄ as precursor. *Coatings* **2018**, *8*, 431. [[CrossRef](#)]
18. Kang, C.; Zhang, C.; Yao, Y.; Yang, Y.; Zong, H.; Zhang, L.; Li, M. Enhanced thermochromic properties of vanadium dioxide (VO₂)/glass heterostructure by inserting a Zr-based thin film metallic glasses (Cu₅₀Zr₅₀) buffer layer. *Appl. Sci.* **2018**, *8*, 1751. [[CrossRef](#)]
19. Houska, J.; Kolenaty, D.; Rezek, J.; Vlcek, J. Characterization of thermochromic VO₂ (prepared at 250 °C) in a wide temperature range by spectroscopic ellipsometry. *Appl. Surf. Sci.* **2017**, *421*, 529–534. [[CrossRef](#)]
20. Vlček, J.; Kolenatý, D.; Houška, J.; Kozák, T.; Čerstvý, R. Controlled reactive HiPIMS—Effective technique for low-temperature (300 °C) synthesis of VO₂ films with semiconductor-to-metal transition. *J. Phys. D Appl. Phys.* **2017**, *50*, 38. [[CrossRef](#)]
21. Choi, Y.; Jung, Y.; Kim, H. Low-temperature deposition of thermochromic VO₂ thin films on glass substrates. *Thin Solid Films* **2016**, *615*, 437–445. [[CrossRef](#)]
22. Fang, M.; Voit, W.; Wu, Y.; Belova, L.; Rao, K.V. In-situ preparation of metal oxide thin films by inkjet printing acetates solutions. *MRS Proc.* **2013**, *1547*, 13–20. [[CrossRef](#)]
23. Peng, Z.; Jiang, W.; Liu, H. Synthesis and electrical properties of tungsten-doped vanadium dioxide nanopowders by thermolysis. *J. Phys. Chem. C* **2007**, *2007* *111*, 1119–1122. [[CrossRef](#)]
24. Zheng, C.; Zhang, J.; Luo, G.; Ye, J.; Wu, M. Preparation of vanadium dioxide powders by thermolysis of a precursor at low temperature. *J. Mater. Sci.* **2000**, *35*, 3425–3429. [[CrossRef](#)]
25. Lee, M.-H.; Kim, M.-G.; Song, H.-K. Thermochromism of rapid thermal annealed VO₂ and Sn-doped VO₂ thin films. *Thin Solid Films* **1996**, *290–291*, 30–33. [[CrossRef](#)]
26. Zhang, H.; Xiao, X.; Lu, X.; Chai, G.; Sun, Y.; Zhan, Y.; Xu, G. A cost-effective method to fabricate VO₂ (M) nanoparticles and films with excellent thermochromic properties. *J. Alloy. Compd.* **2015**, *636*, 106–112. [[CrossRef](#)]
27. Ji, S.; Zhang, F.; Jin, P. Selective formation of VO₂(A) or VO₂(R) polymorph by controlling the hydrothermal pressure. *J. Solid State Chem.* **2011**, *184*, 2285–2292. [[CrossRef](#)]
28. Kam, K.C.; Cheetham, A.K. Thermochromic VO₂ nanorods and other vanadium oxides nanostructures. *Mater. Res. Bull.* **2006**, *41*, 1015–1021. [[CrossRef](#)]

29. Wu, C.; Zhang, X.; Dai, J.; Yang, J.; Wu, Z.; Wei, S.; Xie, Y. Direct hydrothermal synthesis of monoclinic VO₂(M) single-domain nanorods on large scale displaying magnetocaloric effect. *J. Mater. Chem.* **2011**, *21*, 4509. [CrossRef]
30. Malarde, D.; Johnson, I.D.; Godfrey, I.J.; Powell, M.J.; Cibir, G.; Quesada-Cabrera, R.; Palgrave, R.G. Direct and continuous hydrothermal flow synthesis of thermochromic phase pure monoclinic VO₂ nanoparticles. *J. Mater. Chem. C* **2018**, *6*, 11731–11739. [CrossRef]
31. Gagaoudakis, E.; Aperathitis, E.; Binas, V.; Zouridi, L.; Markaki, O.; Kiriakidis, G. Transmission lines thermal switches utilizing novel phase changing materials. In Proceedings of the 2017 52nd International Universities Power Engineering Conference (UPEC) IEEE, Heraklion, Greece, 28–31 August 2017; pp. 1–4. [CrossRef]
32. Li, M.; Magdassi, S.; Gao, Y.; Long, Y. Hydrothermal synthesis of VO₂ polymorphs: Advantages, challenges and prospects for the application of energy efficient smart windows. *Small* **2017**, *13*, 1701147. [CrossRef] [PubMed]
33. Brinker, C.J.; Hurd, A.J.; Schunk, P.R.; Frye, G.C.; Ashley, C.S. Review of sol-gel thin film formation. *J. Non Cryst. Solids* **1992**, *147*, 424–436. [CrossRef]
34. Znaidi, L. Sol-gel-deposited ZnO thin films: A review. *Mater. Sci. Eng. B* **2010**, *174*, 18–30. [CrossRef]
35. Chen, D. Anti-reflection (AR) coatings made by sol-gel processes: A review. *Sol. Energy Mater. Sol. Cells* **2001**, *68*, 313–336. [CrossRef]
36. Madida, I.G.; Simo, A.; Sone, B.; Maity, A.; Kana, J.K.; Gibaud, A.; Merad, G.; Thema, F.T.; Maaza, M. Submicronic VO₂-PVP composites coatings for smart windows applications and solar heat management. *Solar Energy* **2014**, *107*, 758–769. [CrossRef]
37. Salam, A.; Makhlof, H. *Handbook of Smart Coatings for Materials Protection*, 1st ed.; Woodhead Publishing Limited: Cambridge, UK, 2014; ISBN 978-0-85709-680-7.
38. Guglielmi, M.; Kickelbick, G.; Martucci, A. *Sol-Gel Nanocomposites*, 1st ed.; Springer: New York, NY, USA, 2014; ISBN 978-1-4939-1208-7.
39. Chen, Z.; Gao, Y.; Kang, L.; Cao, C.; Chen, S.; Luo, H. Fine crystalline VO₂ nanoparticles: Synthesis, abnormal phase transition temperatures and excellent optical properties of a derived VO₂ nanocomposite foil. *J. Mater. Chem. A* **2014**, *2*, 2718. [CrossRef]
40. Gao, Y.; Wang, S.; Luo, H.; Dai, L.; Cao, C.; Liu, Y.; Chen, Z.; Kanehira, M. Enhanced chemical stability of VO₂ nanoparticles by the formation of SiO₂/VO₂ core/shell structures and the application to transparent and flexible VO₂-based composite foils with excellent thermochromic properties for solar heat control. *Energy Environ. Sci.* **2012**, *5*, 6104. [CrossRef]
41. Lu, Z.; Li, C.; Yin, Y. Synthesis and thermochromic properties of vanadium dioxide colloidal particles. *J. Mater. Chem.* **2011**, *21*, 14776. [CrossRef]
42. Lu, X.; Xiao, X.; Cao, Z.; Zhan, Y.; Cheng, H.; Xu, G. A novel method to modify the color of VO₂-based thermochromic smart films by solution-processed VO₂@SiO₂@Au core-shell nanoparticles. *RSC Adv.* **2016**, *6*, 47249–47257. [CrossRef]
43. Li, S.; Li, Y.; Qian, K.; Ji, S.; Luo, H.; Gao, Y.; Jin, P. Functional fiber mats with tunable diffuse reflectance composed of electrospun VO₂/PVP composite fibers. *ACS Appl. Mater. Interfaces* **2014**, *6*, 9–13. [CrossRef] [PubMed]
44. Wan, M.; Xiong, M.; Li, N.; Liu, B.; Wang, S.; Ching, W.Y.; Zhao, X. Observation of reduced phase transition temperature in N-doped thermochromic film of monoclinic VO₂. *Appl. Surface Sci.* **2017**, *410*, 363–372. [CrossRef]
45. Wyszecki, G.; Stiles, W.S. *Colour Science: Concepts and Methods, Quantitative Data and Formulae*, 2nd ed.; Wiley: New York, NY, USA, 2000; ISBN 978-0-471-39918-6.
46. The Air Mass Coefficient. Available online: [https://en.wikipedia.org/wiki/Air_mass_\(solar_energy\)](https://en.wikipedia.org/wiki/Air_mass_(solar_energy)) (accessed on 19 January 2019).

